Neutron and X-ray Diffraction Study on the Structure of Ultraphosphate Glasses

Uwe Hoppe [1], Günter Walter [1], Dörte Stachel [2], Andrea Barz [2], and Alex C. Hannon [3]

[1] Rostock University, Dept. Physics, D-18051 Rostock
[2] Friedrich Schiller University Jena, Otto Schott Institute, D-07743 Jena
[3] Rutherford Appleton Lab., ISIS Facility, Chilton, Didcot OX11 0QX, UK

Z. Naturforsch. **52a**, 259–269 (1997); received July 6, 1996

The high real-space resolution of neutron diffraction experiments which is provided by use of the epithermal neutrons from spallation sources was exploited in order to differentiate the unlike P–O bonds existing in the PO_4 units of phosphate glass networks. The 2 P–O distance peaks, separated by about 12 pm, which were found in the zinc and the calcium ultraphosphate glasses studied are assigned to oxygen sites on bridging (O_B) and terminal (O_T) positions. The mean P–O distances are nearly invariable versus the growing metal oxide content which results from an elongation of the $P–O_B$ and $P–O_T$ bonds. The bond lengths which are known from the related crystal structures and from ab initio calculations show almost the same behaviour. The discussion of further details of the crystal structures leads to the conclusion that $P–O_B$ rather than $P–O_T$ distances should show more details in case of diffraction measurements of even higher real-space resolution.

The change of the Zn–O coordination number from 6 to 4 versus increasing ZnO content, which was obtained in previous X-ray diffraction experiments, is confirmed by the recent combination of neutron and X-ray diffraction data. On the other hand, the Ca–O coordination number of about 6 is almost invariable.

Key words: Neutron diffraction, X-ray diffraction, Phosphate glasses, Short-range order.

1. Introduction

The PO_4 tetrahedron, known as the basic building unit in phosphate glasses, has 2 considerably different oxygen sites, the terminal (O_T) and the bridging (O_B) oxygen atoms. By O (1 s) X-ray photoelectron spectroscopy (XPS) the fractions of both species were determined in a large range of composition beginning from vitreous (v-)P_2O_5 [1–3]. The results confirm the depolymerization effect of metal oxide additions. Van Wazer [4] has predicted that binary distributions of Q^n species should be formed in phosphate glasses. Even that was repeatedly proved by ^{31}P magic angle spinning (MAS) NMR [2, 5]. Q^n means a PO_4 unit with a number n of links. Thus, in the range between v-P_2O_5 (only Q^3 groups) and the metaphosphate systems (only Q^2 groups) the networks of ultraphosphate glasses are constituted from Q^3 and Q^2 units.

The Q_T atom on the unlinked vertex of the Q^3 unit is doubly bonded, so it is called an O_{DB} atom. From the lack of any experimental evidence which would suggest to distinguish between a $P–O^{(-)}$ bond and a $P=O$ bond in the Q^2 middle group it was concluded to assign the double-bond character partially to both O_T atoms of this tetrahedron [2]. Hence, both terminal oxygens of the middle group are termed non-bridging ones (O_{NB}).

Since all of the $P–O_T$ bonds carry a p–d π-character in addition to their σ-character, the respective bond lengths appear much shorter than $P–O_B$ distances. Studies of such distance differences and their subtle changes are a domain of neutron diffraction experiments performed on spallation sources. This method provides an extensive measuring range of momentum transfer $Q = 4\pi/\lambda \sin\theta$ up to 400 nm^{-1} and more, where λ is the radiation wavelength and 2θ is the scattering angle. Previously, measurements of that high real-space resolution were performed on sodium [6] and potassium [7] metaphosphate glasses. The experiments revealed a clear splitting effect of the P–O first neighbour peak into 2 equal contributions which were related with the numbers of $2\,O_{NB}$ and $2\,O_B$ atoms existing in the PO_4 middle group. The distance differences were found to diminish under the influence of modifier cations of high electric field strength like Pb^{2+}, Zn^{2+}, Mg^{2+} or Al^{3+} [8] but the splitting is still obvious. Up to now, this effect was not examined in ultraphosphate glasses, even not in v-P_2O_5. Taking

Reprint requests to Dr. U. Hoppe; Fax: 03 81 4 98 17 26.

0932-0784 / 97 / 0300-0259 $ 06.00 © – Verlag der Zeitschrift für Naturforschung, D-72072 Tübingen

into account the O (1 s) XPS results mentioned above [1–3] a double peak of the P–O distances should exist in the ultraphosphate range, as well.

The question about a further differentiation of bond lengths in ultraphosphate glasses can be discussed on the basis of related crystalline structures. From $P-O_T$ distances known for ultraphosphate crystals it was concluded [9] that the difference between $P-O_{DB}$ bond lengths in Q^3 groups and $P-O_{NB}$ distances in Q^2 groups should not be detectable. A consideration of P–O bond lengths in the interplay between both Q^n species and the cations is planned.

Surprisingly, the mean P–O bond lengths in phosphate glasses show only very slight alterations with the metal oxide content. By use of X-ray diffraction (XRD) measurements, mean P–O distances of about 155 pm were obtained for v-P_2O_5 [10] and for a series of Mg phosphate glasses [11]. The same observations were made for series of Zn, Ca, and Ba phosphate glasses [12]. Thus the ratio of bonds $n(P-O_B)/n(P-O_T)$ diminishes from 3 to 1 for molar ratios $y = n(MeO)/n(P_2O_5)$ from 0 to 1.0, i.e., the various species of P–O bond lengths themself must increase with growing metal oxide content. Such a change might compensate for the enhanced fraction of the short $P-O_T$ bonds.

The results about Me-O coordination numbers in ultraphosphate glasses from previous XRD experiments [11, 12] contain uncertainties. For example, the Ca–O distance peaks are superimposed with O–O contributions. In the evaluation of N_{MeO} values from the XRD data [11, 12] the area of the O–O peak was chosen according to the expected value $N_{OO} = 24/(5 + y)$, and the O–O distances were fixed. The use of complementary results, i.e. combination of neutron diffraction and XRD data, will improve the reliability of the Me-O coordination numbers. The gain by this method was demonstrated studying N_{MeO} values in various metaphosphate glasses [13]. Such a combination will be applied in the present study.

In order to explain the changes of Me-O coordination numbers and packing densities found in ultraphosphate glasses a mechanism was suggested where Me-O-P bridges play an eminent role [12]. In a definite compositional range the values of N_{MeO} diminish, which was interpreted as to maintain the formation of Me-O-P bridges. However, a stabilization of such bridges is abnormal for network-modifier cations. The covalent component of Me-O bonds was suggested to be responsible for this effect [9]. Thus, a comparison of the behaviour of N_{ZnO} and N_{CaO} is of special interest. These network-modifier atoms show different covalent contributions to the Me-O interactions. Glasses with 25 mol%, 33 mol%, and 40 mol% MeO content were chosen for the experiments. The available numbers N_{MeO} of metaphosphate glasses (50 mol% MeO) [13] are of sufficient quality for the discussion.

2. Experimental

2.1 Sample Preparation

The samples of calcium and zinc ultraphosphate glasses studied were chosen for their moderate stability against moisture attack. Due to the high incoherent scattering of hydrogen in neutron diffraction experiments any contamination of the samples with H_2O would be more prejudical to a correct calibration of the curves than to the subsequent considerations on structural data. Thus, the sample preparation which is described elsewhere [14] needs extensive care to minimize the water incorporation. The raw materials of the glasses, P_4O_{10} (p.a., Merck) and the powdered and dried metaphosphates (Piesteritz), were loaded into silica ampoules which subsequently were sealed. After a preheating process, the melts in the ampoules were held at 1050 °C for 2 hours. The ampoules were broken after cooling, and pieces of the sample material were kept in carbon tetrachloride to avoid moisture attack. The compositions were determined by means of an electron microprobe X-ray analyzer. The molar ratios $y = n(MeO)/n(P_2O_5)$ of the 5 glasses studied were 0.330, 0.497, and 0.658 with Me = Ca, and 0.502 and 0.678 with Me = Zn. The mass densities of the samples, given in the same order as above, were 2.450, 2.453, 2.488, 2.80, and 2.81 gcm^{-3}, respectively.

2.2 Diffraction Experiments

The neutron diffraction experiments were performed using the time-of-flight technique on the LAD diffractometer at the ISIS pulsed neutron source at Rutherford Appleton Laboratory. The dried and crushed pieces of glass were loaded into vanadium containers of 11 mm in diameter. During the data collection, which takes about 15 hours in every sample run, the vanadium can was located in a vacuum chamber. The incident neutron spectrum was determined by help of a vanadium rod. The data were

corrected by standard procedures for attenuation, multiple scattering, inelasticity effects, and for container and background scattering [15]. Difficulties of the normalization in the range of low energy neutrons (< 50 meV) might be ascribed to a slight contamination of the samples by atmospheric humidity.

The complementary XRD measurements were performed using a step scan mode on a horizontal goniometer which was setted at an X-ray generator with a rotating silver anode. The sample containers used were thin-walled capillaries made of silica with about 0.9 mm in diameter. The scans were performed up to an angle 2θ of 130°, which in all leads to a measuring range in Q from 4 nm^{-1} up to 202 nm^{-1}. A crystal monochromator was positioned in the incident beam. In case of the zinc phosphate glasses, a filter was applied to suppress the fluorescence radiation in the diffracted beam. The correction procedures used are described in [10, 11].

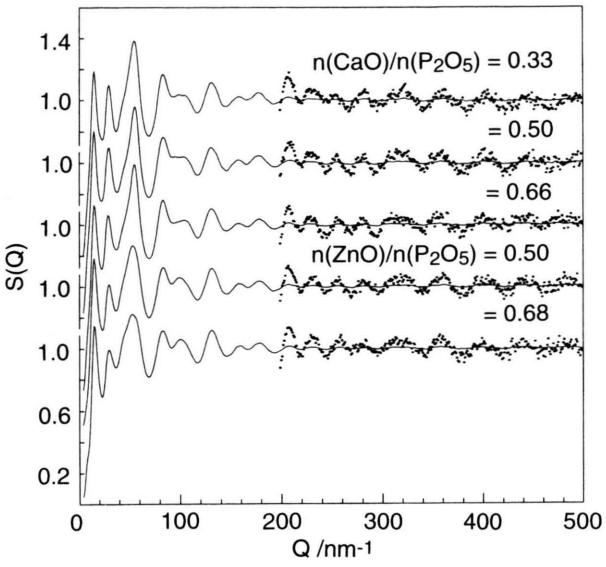

Fig. 1. Experimental neutron structure factors of the samples studied. Compositions are indicated in the plot. Beyond $Q = 200$ nm^{-1} the oscillations are 8 times enhanced to make obvious the interferences in the high-Q range.

3. Results

The normalized differential scattering cross-sections, $d\sigma/d\Omega$, obtained by the neutron diffraction experiments were converted into the Faber-Ziman structure factors, $S_N(Q)$, by

$$S_N(Q) = \frac{\frac{d\sigma}{d\Omega} - [\langle b^2\rangle - \langle b\rangle^2]}{\langle b\rangle^2}, \qquad (1)$$

where b_i is the neutron scattering length of atoms of sort i and $\langle\ldots\rangle$ means the average with respect of the sample composition. In the case of XRD, the normalized intensities were expressed in the same notation, where the X-ray form factor, $f_i(Q)$, stands instead of the value b_i. The $S_X(Q)$ curves of the calcium phosphate glasses show some incorrect features in the range $Q > 180$ nm^{-1}.

The neutron structure factors of all of the 5 samples studied are shown in Figure 1. The oscillations, which are plotted as points in the high-Q range of the $S(Q)$ curves, were amplified for better visibility. They demonstrate the profitableness of measurements up to Q of 500 nm^{-1}. The interferences caused by the P–O bond distances dominate the scattering result in the range of $Q > 300$ nm^{-1}. This was illustrated by a comparison of the experimental interferences with the backtransform of those 2 Gaussian curves which model the P–O distance peak [7]. Such curves $Q[S_N(Q) - 1]$ were presented in Fig. 3 of [7] for a KPO_3 glass which was studied under the same conditions as described here.

On a first view, the oscillations in the high-Q range of Fig. 1 seem to be very similar for all of the samples studied. Slight variations in the $S(Q)$ functions must contain that information which reflects the progress of the network depolymerization, e.g. the increase of the fraction of the short $P-O_T$ bonds at the expense of the $P-O_B$ contribution. This effect will become more obvious in the total real-space correlation functions, $T(r)$, which were obtained by

$$T(r) = 4\pi r \varrho_0 + 2/\pi \int_0^{Q_{max}} M(Q)\,[S(Q) - 1]\sin(Q\,r)\,Q\,dQ\,. \qquad (2)$$

Here ϱ_0 is the number density of atoms. $M(Q)$ stands for the Lorch modification which was applied in the calculations of the total correlation functions $T_X(r)$. Thereby the values of Q_{max} were 175 nm^{-1} and 202 nm^{-1} for the calcium and zinc glasses, respectively. Despite the noticeable statistical error present in the experimental $S_N(Q)$ curves at high Q, the respective Fourier transformations were performed up to 500 nm^{-1} without any modifications of the data. The distance ranges in the $T(r)$ functions showing the P–O, Me-O, and O–O peaks are plotted in Fig. 2

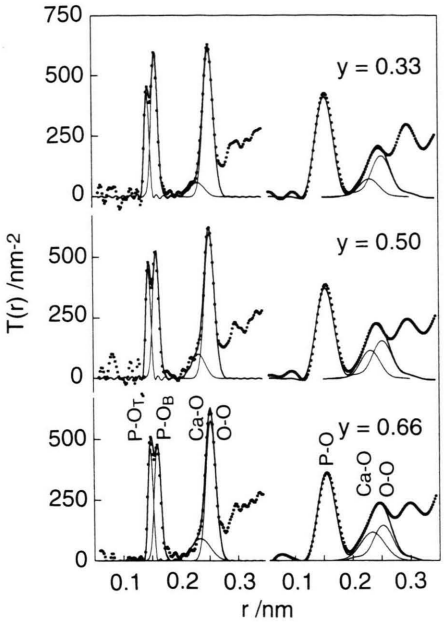

Fig. 2. Real-space correlation functions, $T(r)$, of three calcium ultraphosphate glasses, studied by neutron diffraction – on the left; by XRD – on the right (experimental curves – dotted lines; fitted model peaks – thin solid lines; their sum – thick solid lines). The molar ratios are indicated in the plot. In the calculations according to (2) the upper integration limits used were $Q_{max} = 500\ nm^{-1}$ (neutron diffraction) and $175\ nm^{-1}$ (XRD). In case of XRD the Lorch modification was applied.

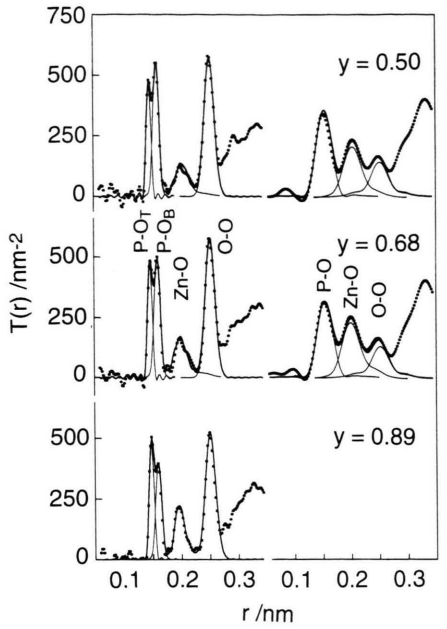

Fig. 3. As Fig. 2, but in the calculation according to (2) the upper integration limit used for XRD was $202\ nm^{-1}$ (XRD). The single curve belongs to results of a $ZnO-MgO-P_2O_5$ glass in [8].

($CaO-P_2O_5$ glasses) and in Fig. 3 ($ZnO-P_2O_5$ systems). In Fig. 3 the curves of a previous measurement on a ternary glass [8] are included. This sample has approximately metaphosphate composition. A splitting of the P–O peak into 2 contributions is obtained in all the glasses studied. Moreover, the raising peak of the $P-O_T$ distances the number of which grows with increasing MeO content at the expense of the $P-O_B$ bonds, is obvious.

In the evaluation of parameters of the P–O bond distances the corresponding peak was modelled by two Gaussian profiles, where the coordination number, the mean distance and the full width at half maximum (fwhm) were the adjustable parameters used. According to the knowledge from previous XRD measurements [12], Ca–O distances can be approximated by a single peak while for the Zn–O distances a second peak at 235 pm has to be taken into account. An evident contribution in this distance range is the O–O peak which belongs to the edges of the PO_4 tetrahedra. The least-squares fits of the distance peaks were simultaneously performed, including both the neutron and the X-ray $T(r)$ functions. This combination allows a reliable differentiation of the superimposing Me–O and O–O distances.

Only in consideration of the termination effect of the Fourier integral in (2) the least-squares fit procedure can lead to reliable results. A procedure according to suggestions of Waser & Schomaker [16], also described by Wright & Leadbetter [17], was applied, where the model peaks, i.e. the Gaussian profiles, were folded with so-called peak functions $P_{ij}(t)$. Here the appropriate function belonging to the X-ray data is given by

$$P_{ij}(t) = 1/\pi \int_0^{Q_{max}} \frac{f_i(Q)\, f_j(Q)}{\langle f \rangle^2} M(Q) \cos(Q\, t)\, dQ\,. \qquad (3)$$

The total model correlation function, $T_{mod}(r)$, is obtained by

$$T_{mod}(r) = \Sigma_i \Sigma_j c_i \int_0^{\infty} T_{ij}(t)\,[P_{ij}(r-t) - P_{ij}(r+t)]\, dt\,, \quad (4)$$

where curves $T_{ij}(t)$ are composed of Gaussian profiles. c_i is the mole fraction of atoms i.

The neutron and X-ray $T(r)$ functions were obtained using very different upper integration limits Q_{max}. According to the small width of $P_{PO}(t)$ of 7.6 pm ($\Delta r \cong 3.79/Q_{max}$) in case of the neutron data only a slight broadening is introduced. Hence, details of the P–O bond were predominantly determined by the $T_N(r)$ curve from the neutron data. But the same model peaks fit approximately the distance peak at $r = 155$ pm in the $T_X(r)$ curves. Here the width of the $P_{PO}(t)$ function is 26.9 pm if Q_{max} is assumed to be 202 nm^{-1} and the Lorch modification is taken into account ($\Delta r \cong 5.44/Q_{max}$).

The resulting parameters of the fit procedures which correspond to the model Gaussian curves are given in Table 1. Note that the various model peaks shown in Figs. 2 and 3 are already broadened by folding them with the peak functions $P_{ij}(t)$. Ripples caused by the termination effect are only visible near the P–O peaks of the $T_N(r)$ functions because the width of these model peaks (about 10 pm) is of similar magnitude as that additionally introduced by the termination effect. Thus, if one exceeds Q_{max} of 300 nm^{-1}, the gain in information mainly concerns the P–O peaks. Note, the Lorch modification, applied on the X-ray data, suppresses these ripples in the corresponding curves.

Reliable parameters of the Me–O peak could be determined. The single distance peak at 250 pm in the $T(r)$ functions of the $CaO\text{-}P_2O_5$ glasses (Fig. 2) was separated into the contributions from the Ca–O and O–O peak. In the zinc phosphate glasses studied (Fig. 3) the tail of the Zn–O peak formed by a weak second distance is an obvious feature of the Zn–O environments. The reasonable number of Gaussian profiles here applied restricts the interpretation to those parameters which are given in Table 1. Further refinements of the distance distributions might be of interest, e.g. the use of other than Gaussian profiles, but this task is out of the limit of the quality of the data. The obvious ripples in the neutron $T(r)$ curves, which in the low-r range exceed in amplitude the termination ripples, are a signature for certain small systematic errors in the experimental data.

Table 1. Peak fit parameter for the ultraphosphate glasses studied (On the right hand – total coordination numbers and mean distances).

Atom pair	Coordination number	Distance (in pm)	fwhm (in pm)	Coordination number	Distance (in pm)
$y = 0.330$					
P–O	1.30 (5)	145.3 (10)	9.5 (10)	3.97 (10)	154.4 (5)
	2.67 (5)	158.8 (10)	13.0 (15)		
Ca–O	5.5 (8)	232 (2)	30 (5)		
O–O	4.45 (20)	252.0 (19)	20 (2)		
$y = 0.497$					
P–O	1.45 (5)	145.7 (10)	9.4 (10)	3.90 (10)	154.2 (5)
	2.45 (5)	159.2 (10)	13.0 (15)		
Ca–O	6.1 (5)	232 (2)	28 (5)		
O–O	4.34 (20)	252.0 (10)	20 (2)		
$y = 0.658$					
P–O	1.63 (5)	147.5 (10)	10.0 (10)	4.03 (10)	154.9 (5)
	2.40 (5)	160.0 (10)	13.5 (15)		
Ca–O	6.2 (4)	234 (2)	40 (5)		
O–O	4.20 (20)	252.3 (10)	20 (2)		
$y = 0.502$					
P–O	1.45 (5)	146.0 (10)	9.0 (10)	3.93 (10)	154.2 (5)
	2.48 (5)	159.0 (10)	12.1 (15)		
Zn–O	5.7 (3)	203 (2)	27 (2)		
	1.4 (5)	235*	50 (5)		
O–O	4.25 (20)	251.8 (10)	21 (2)		
$y = 0.678$					
P–O	1.55 (5)	146.5 (10)	9.0 (10)	3.93 (10)	154.4 (5)
	2.38 (5)	159.5 (10)	12.5 (15)		
Zn–O	5.2 (3)	199 (2)	25 (2)		
	1.3 (5)	235*	44 (5)		
O–O	4.20 (20)	251.9 (10)	20 (2)		

* Parameter was fixed during the fit.

4. Discussion

4.1 The 2 Separate P–O Distance Peaks Observed

The excellent resolution of the real-space correlation functions makes it possible to discuss the $P\text{–}O_T$ and $P\text{–}O_B$ bond lengths in their dependence on the modifier content. In order to enlarge the considered compositional range, the data of 4 other glasses will be used, too. Among these glasses, the 2 P–O bonds were separated only for the $ZnO\text{-}MgO\text{-}P_2O_5$ system [8]. The total P–O coordination numbers and the mean P–O distances, together with the parameters belonging to the $P\text{–}O_T$ and the $P\text{–}O_B$ contributions for all of the 5 samples studied and for the 4 additional glasses, are plotted in Figure 4. In the upper part of the plot straight lines indicate the expected behaviour of coordination numbers. Due to the conversion of Q^3 into Q^2, groups the N_{PO} should alter according to $1 + y$ and $3 - y$ for the O_T and the O_B atoms, respectively, where y is the molar ratio $n(MeO)/n(P_2O_5)$. The fraction of Q^2 is equal to this ratio up to $y = 1$ [2, 5]. The experimental values of both P–O contributions

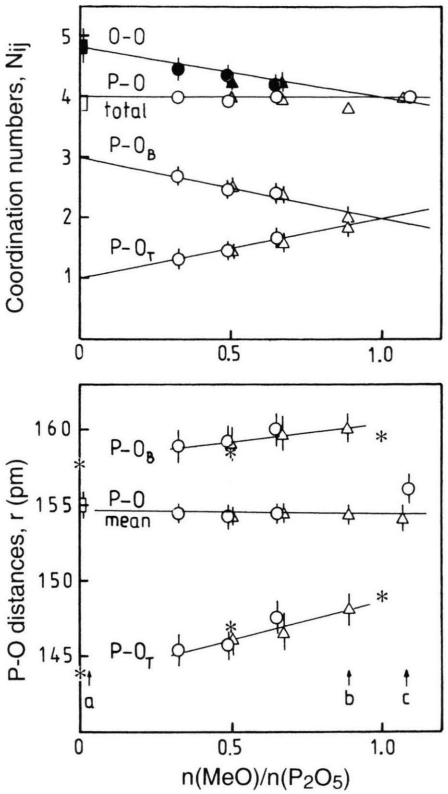

Fig. 4. Coordination numbers and distances belonging to the O_B and O_T contributions to the P–O bond. Triangles correspond to the $ZnO-P_2O_5$ systems; circles denote values of the $CaO-P_2O_5$ systems; the square means v-P_2O_5. Lines in the upper plot mark the expected behaviour. Full markers indicate the O–O coordination numbers. The lines in the lower plot are guides to the eye. Values at compositions marked by arrows and letters a, b, and c denote values taken from [10], [8], and [13], respectively. The asterisks mark values taken from ab initio calculations [26].

agree well with the expected curves. Additionally, the O–O coordination numbers are plotted. Their behaviour expresses the progress of the network depolymerization by a weak decrease according to $N_{OO} = 24/(5 + y)$ [11]. This formula reflects that an O_B atom has 6, an O_T atom only 3 nearest oxygen neighbours.

The mean P–O distances which are shown in the lower part of Fig. 4, confirm the observations from our previous XRD studies on ultraphosphate glasses [11, 12]. Their values do not depend on the metal oxide content. This finding might explain why the periods of oscillations in the high-Q range of all of the neutron structure factors shown in Fig. 1 appear almost independent of composition. Since the fractions of both contributing bonds vary continuously, a further effect must compensate for the increasing component of the short $P-O_T$ distances. The explanation is found in the increase of both distances, $P-O_T$ and $P-O_B$, with growing MeO content. The elongation is stronger for the $P-O_T$ bonds.

The respective details will be checked in related crystal structures [18–25]. Moreover, it is possible to make use of the results from ab initio molecular orbital (MO) calculations (Uchino and Ogata [26]). These MO calculations were performed on 3 pairs of Q^n groups. The authors suggested their results to be valid for v-P_2O_5 and for 33 mol% and 50 mol% sodium phosphate glasses. The mean P–O distances and the 2 separate contributions, which were obtained in the PO_4 units of the crystals and the clusters, are given in Table 2. Actually, the mean P–O distances of the crystals and clusters are quite independent of the composition, such as found in previous XRD measurements [10–12]. The 2 distances, $P-O_T$ and $P-O_B$, from the MO calculations [26] are plotted in Fig. 4 as asterisks. Both values well reproduce the behaviour here observed. The elongation of the $P-O_T$ bonds is also found in the related crystal structures. However, their $P-O_B$ distances do not show a clear trend. The difference of the $P-O_T$ and $P-O_B$ distances is largest in the P_4O_{10} crystal [18], due to the kind of packing of the P_4O_{10} molecules showing the most open environments of the O_{DB} positions.

For obvious reasons, the P–O bond lengths in a Q^2 group might be assumed to be larger than those in Q^3.

Table 2. Mean P–O distances and the $P-O_T$ and $P-O_B$ distances in selected phosphate crystals and in clusters obtained by MO calculations [26]. Distance values are given in pm.

Chemical formula	Fraction of Q^2 units	P–O	$P-O_T$	$P-O_B$	Ref.
P_4O_{10}	0.0	155.0	143.2	159.0	[18]
P_2O_5 II	0.0	154.3	144.5	157.6	[19]
P_2O_5 III	0.0	153.9	144.4	157.0	[20]
ZnP_4O_{11}	0.5	153.6	145.7	158.3	[21]
CaP_4O_{11}	0.5	153.9	145.0	159.2	[22]
NdP_5O_{14}	0.6	153.8	146.7	158.5	[23]
$Ca_2P_6O_{17}$	0.66	153.7	147.2	158.4	[24]
CaP_2O_6	1.0	153.2	148.3	158.2	[25]
$H_4P_2O_7$	0.0	154.2	143.9	157.7	[26]
$H_3P_2O_7Na$	0.5	154.2	146.9	158.6	[26]
$H_2P_2O_7Na_2$	1.0	154.2	148.9	159.5	[26]

Predominantly this might be connected with the fact that in the Q^2 group the p-d π-bond character is shared between 2 $P-O_T$ bonds. In accordance with the growing fraction of Q^2, this would give a simple explanation for the elongation of the $P-O_T$ bonds.

4.2 Consideration on Further Details of P–O Distances

In order to clarify the contributions of Q^3 and Q^2 groups to the P–O bond lengths, even more details about the crystalline structures and the cluster configurations than have been shown in Table 2, can be evaluated. Some of the corresponding details could become visible if even higher real-space resolution in the diffraction experiments could be achieved. Therefore, the P–O bonds were considered in respect of their location either in Q^3 or in Q^2 groups. Furthermore, both species of $P-O_B$ bonds are part of a link either with a Q^3 or with a Q^2 group. The corresponding lengths, given in Table 3, are mean values of various equivalent bonds.

The $P-O_T$ distances in the clusters reveal two values of unlike O_T positions, those in Q^3 or Q^2 groups, while the corresponding values are hardly to differentiate in the crystals. This may be caused by a definite defect of the $H_3P_2O_7Na$ cluster, where the O_{DB} atom is not coordinated by a modifier cation. This fact is in contradiction to the related MeP_4O_{11} crystals and to a structural conception of ultraphosphate glasses [9] which was concluded from Me-O coordination numbers (XRD results) and packing densities [12] (see also Section 4.4). In phosphate glasses of 33 mol% metal oxide content, almost all of the O_{DB} atoms should have a cation neighbour. The interaction with a cation has consequences for the $P-O_T$ bond lengths. Hence, the $P-O_{DB}$ and the $P-O_{NB}$ bonds are of equal length. Only in glasses with very low modifier content a second species of $P-O_T$ bond, belonging to those O_{DB} atoms which, typically for v-P_2O_5, have no adjacent cation, can appear. Up to now such a bond length was not determined. Thus, a detection of separate species of $P-O_T$ bonds, in Q^3 and Q^2 groups, is generally impossible in the glasses studied.

The $P-O_B$ distances are little different within all those P–O–P bridges of clusters and crystals where equal Q^n species are linked (cf. Table 3). Those values of the $H_3P_2O_7Na$ cluster which are setted in parenthesis may be considered as such distances, too. Pairs of like Q^n are common in v-P_2O_5 and in the metaphosphate systems, both glasses formed from only one species of Q^n. The networks of the ultraphosphate crystals contain a reasonable amount of links between unlike Q^n species. In such a P–O–P bridge, the $P-O_B$ bond in the Q^2 group is lengthened while that in the Q^3 group is shortened. A Q^3-Q^2 pair of a ZnP_4O_{11} crystal [21] is illustrated in Fig. 5, where all the distance values are indicated. Here the qualitative considerations, which were made concerning the bond lengths in Q^2 groups should be remembered. The effect of adjacent cations modifies the P–O bonds [7, 8]. Changes of P–O bond lengths were explained by slight shifts of electron density. A bond is shortened if the electron density is shifted along the bond from the more positive to the more negative partner, and vice versa (Gutmann [27]). Accordingly, the following is suggested for explanation of the various $P-O_B$ bond lengths given in Table 3: Since in a P–O bond oxygen atoms are negatively, the P atoms are positively charged, the changes of lengths in P–O–P bridges in Q^3-Q^2 pairs indicate a shift of electron density from the Q^2 to the Q^3 group. The O_{NB} atoms of the Q^2 group carry the counter charge of the metal cation, i.e. an excess of electron density. Obviously, this charge tends to distribute on the remaining network. The arrows in Fig. 5 mark the shifts of negative charges. Such a tendency would indicate a preference of links between the Q^3 and the Q^2 group.

The charge transfer indicated in Fig. 5 weakens the π-bond to the O_{DB} atom in the Q^3 group, while such a bond character is strengthened to the O_{NB} sites in

Table 3. Classification of P–O bond lengths in those phosphate crystals and small clusters already presented in Table 2. The various bonds are classified according to their positions in Q^n groups, the $P-O_B$ bonds additionally according to their directions of links. Distance values are given in pm. Values in parentheses denote lengths of bonds to oxygen atoms whose second valencies are saturated by a hydrogen atom.

Chemical formula	Fraction of Q^2	$P-O_T$		$P-O_B$ in Q^3		$P-O_B$ in Q^2	
		Q^3	Q^2	$\Rightarrow Q^3$	$\Rightarrow Q^2$	$\Rightarrow Q^3$	$\Rightarrow Q^2$
P_4O_{10}	0	143.3	–	159.0	–	–	–
P_2O_5 II	0	144.5	–	157.6	–	–	–
P_2O_5 III	0	144.4	–	157.0	–	–	–
ZnP_4O_{11}	0.5	145	146	157	155.5	162	–
CaP_4O_{11}	0.5	144.5	145	159	155.5	163	–
NdP_5O_{14}	0.6	146	147	–	156	161	–
$Ca_2P_6O_{17}$	0.66	146	147.5	–	156	161	158
CaP_2O_6	1.0	–	148.3	–	–	–	158.2
$H_4P_2O_7$	0	143.9	–	157.7	–	–	–
$H_3P_2O_7Na$	0.5	144.2	148.3	(158.3)	156.2	161.2	(158.6)
$H_2P_2O_7Na_2$	1.0	–	148.9	–	–	–	159.5

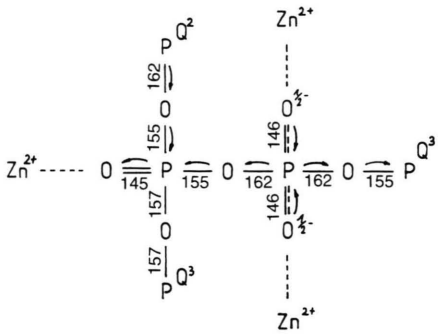

Fig. 5. A Q^3–Q^2 pair in a ZnP_4O_{11} crystal [21]. The nominal charges introduced by the breakage of the P–O–P bridges due to MeO additions are indicated on the O_{NB} sites of the Q^2 group. The arrows mark the directions of shifts of negative charge toward the O_{DB} sites on adjacent Q^3 groups. Bond lengths are given in pm.

the Q^2 groups. Hence, all P–O_T bonds are equalized. However, according to the progress in the conversion of Q^3 to Q^2, the total amount of π-character per P–O_T distance is diminished. The mean value of P–O_T distances increases in this process.

4.3 Prefered Links Between Unlike Q^n Species

The conception about the overall spread of negativ charges from the O_{NB} atoms toward the rest of the anionic network-former skeleton (Sect. 4.2) is in agreement with conclusions drawn from MO calculations by Uchino et al. [28] and with suggestions of Duffy et al. [29] which concern the charge distribution in their optical basicity model. As quoted above, the O_{DB} of the Q^3 group tends to coordinate a modifier cation [9, 12]. Hence, Q^3 groups approach the positions of modifier cations. Furthermore, for reasons of charge compensation the Q^2 groups are first neighbours of the cations. The following is suggested: The electron shift, which was indicated by the alterations of the P–O bond lengths, reflects the local improvement of the charge compensation. The distribution of the excess of electron density smeared at the PO_4 units around the point charge of the cation sites screens the modifier positions most effectively. That improves the ionic bonding. Thus, prefered links are formed between unlike Q^n units such that the negativ charge of the Q^2 can be widely spread. A direct experimental evidence of such links was given by the ^{31}P two-dimensional (2D) MAS NMR [30]. An almost alternating arrangement of Q^3 and Q^2 group was proposed to exist in the 36 mol% sodium phosphate glass studied.

If every of the Q^n would prefer links with the groups of the other sort, definite compositions of ultraphosphate glasses could be determined whereby "regular" arrangements of the Q^n species with uniform environments of all of the Q^3 and the Q^2 would be formed. This concept is similar to the model about the degradation of the Q^3 network of Reiss and Stachel [31]. They predicted that every Q^3 group tends to link with at first one Q^2, then two Q^2, and so forth. Here 4 compositions of uniform Q^n environments were found to be possible. The respective numbers of adjacent groups are specified in Table 4. Typical sections of the respective networks are shown in Figure 6. Regular arrangements may indicate the formation of crystal structures. Actually, ultraphosphate crystals whose structures show links as predicted in Fig. 6 are known for Me^{2+} cations at $y = 0.5$ [21, 22], and for Me^{3+} at $y = 0.6$ [23].

The composition of the glass sample studied by ^{31}P 2D NMR [30] is equivalent that with $y = 0.6$ (37.5 mol% Na_2O). Thus, the dominance of Q^3–Q^2 neighbours observed in the sodium ultraphosphate glass [30] matches with the suggested regular pattern of links. In the P–O–P bridges between the unlike Q^n groups two different P–O_B distances are formed (cf. in Table 3 the data about the NdP_5O_{14} crystal with a distance difference of 5 pm). By the diffraction experiment presented here it is not possible to resolve lengths of this magnitude. Just as high field strengths of cations broaden the widths of the P–O_T and the

Table 4. Number of Q^n species linked with the Q^3 and the Q^2 groups of those 4 ratios $n(Q^2)/n(Q^3)$ of ultraphosphate compositions $y = n(MeO)/n(P_2O_5)$ whose Q^n can be arranged in uniform environments. Compare for illustration the drawings in Figure 6.

Ratio $n(Q^2)/n(Q^3)$	Composition y	Number of Q^n neighbours around the			
		Q^3 group		Q^2 group	
		Q^3	Q^2	Q^3	Q^2
v-P_2O_5	0.0	3	0	–	–
0.5	0.33	2	1	2	0
1.0	0.50	1	2	2	0
1.5	0.60	0	3	2	0
3.0	0.75	0	3	1	1
$Me(PO_3)_2$	1.0	–	–	0	2

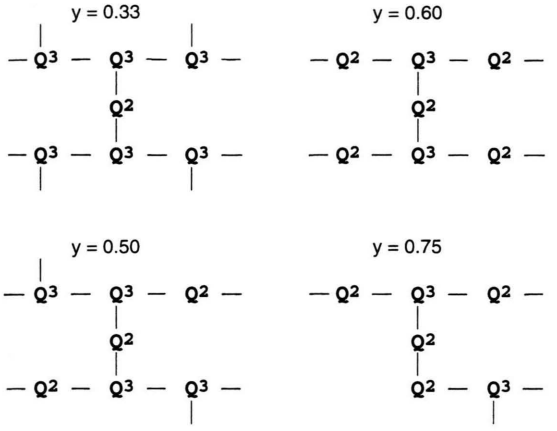

Fig. 6. Schematic drawings of small moieties which show the neighbours of Q^3 and Q^2 groups for those ultraphosphate compositions $y = n(\mathrm{MeO})/n(\mathrm{P_2O_5})$ whose Q^n groups can appear in uniform environments. The preference of pairs of unlike Q^n is taken into account.

$P-O_B$ distance peaks [7, 8], the fwhm of the various $P-O_B$ peaks observed by the present experiments cannot be exploited to estimate different $P-O_B$ distances.

The valence electrons of cations from modifier atoms of low electronegativity pass completely to the anionic network. Thus, the effect of pairing of unlike Q^n groups should be pronounced in such glasses. Moreover, in case of cations of low electric field strength their effect on the lengths of the P–O bonds is small. That leads to the smallest widths of the distance peaks of the various P–O bond species. Thus, in order to see more details of the P–O bonds than in the present study, diffraction experiments on alkali ultraphosphate glasses should be performed.

4.4 The Me–O Environments

In ultraphosphate glasses of low metal oxide content the modifier cations act on the network as an ingredient of re-polymerization [9]. This process starts in v-P_2O_5 with 40% of the oxygen atoms, the doubly bonded ones, being singly coordinated. The incorporation of one MeO produces two additional O_T sites. But one Me^{2+} cation satisfies the coordination of commonly 4 or more O_T atoms. Thus, the surfeit of the terminal oxygens compared with the coordination capability of modifier cations will be lost. At a definite composition, where the ratio $M_{TO} = n(O_T)/n(\mathrm{Me})$ is diminished to the coordination number, N_{MeO}, the re-polymerization is finished. For bivalent Me the corresponding value M_{TO} [12] is given by

$$M_{TO} = 2(y + 1)/y \,. \tag{5}$$

Beginning at this point the MeO_n polyhedra, which at first are preferably in isolated positions and surrounded by Me–O–P bridges, link together by vertices, edges, and faces. Between both compositional ranges a further one appears if the N_{MeO} values are varied. This effect should arise in glasses with such Me–O bonds which exhibit a slightly covalent character and which, therefore, can stabilize Me–O–P bridges. Minima positions of packing densities indicate the upper limit of this range which was called a range II in [9]. The inefficient packing is attributable to low N_{MeO} values as well as to the dominance of oxygen bridges. Such minima were observed in calcium and zinc phosphate glasses at the compositions $y = 0.5$ and 1.0 [12], which correspond to Me–O coordination numbers of 6 and 4, respectively, according to (5).

Actually, the predicted values of Me–O coordination numbers were found at the concerning glass compositions [12]. However, N_{MeO} values of 6 and 4 for Ca and Zn, respectively, are quite common in oxide glasses. More arguments for the hypothesis about the formation of Me–O–P bridges should be given. If in a certain compositional range the N_{MeO} values behave equivalent to the amount of available O_T atoms (M_{TO}), then the respective conclusions can be drawn. The previous XRD results [12] indicated such a behaviour for Ca^{2+} between $y = 0.3$ and 0.5, and for Zn^{2+} between $y = 0.5$ and 1.0. This is illustrated in Fig. 7 by a comparison of N_{MeO} values (small filled circles) with the values of M_{TO} (dashed curves).

The N_{ZnO} values of the phosphate glasses studied corroborate the existence of a behaviour according to range II [9]. The new Zn–O coordination numbers which are plotted as hollow circles at $y = 0.5$ and 0.66, well follow the numbers of available terminal oxygen atoms per metal cation. Thereby we will not stress the reliability of the tails in the Zn–O peaks (cf. Fig. 3) which lead to total N_{ZnO} values marked by the x signs in Figure 7. The tails indicate an asymmetric component in the Zn–O distance peaks. Due to the correct separation of the O–O contributions from the Zn–O peaks, the present results are of even better quality than the previous XRD data [12]. Thus, up to the metaphosphate composition, Zn^{2+} cations are preferably surrounded by Zn–O–P bridges with the O_{DB} atoms of the Q^3 groups incorporated in their environ-

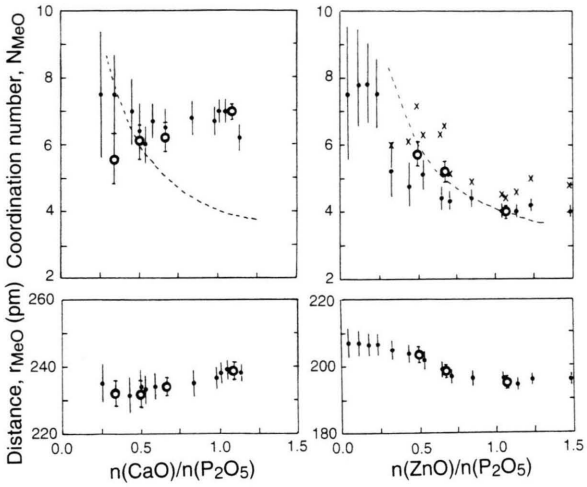

Fig. 7. Comparison of Me–O coordination numbers and Me–O distances from a combination of neutron diffraction and XRD results of the ultraphosphate glasses studied and metaphosphate glasses [13] (hollow circles) with values from previous XRD studies [12] (small full circles). The dashed lines denote the ratio $M_{TO} = n(O_T)/n(Me)$. The x signs on the right plot give total N_{ZnO} values, taking into account the weak contributions of a small second peak.

ments. The Zn–O distances which are plotted in Fig. 7 (buttom) confirm the alterations of the N_{ZnO} values. Just below $y = 0.5$, the values r_{ZnO} start to decrease from 207 pm to about 195 pm at the metaphosphate composition.

In [9, 12] it was assumed for glasses of low MeO content that due to the coordination tendency of the O_{DB} atoms large Me–O coordination numbers should exist. Thus, according to (5) in the glass of 25 mol% CaO ($y = 0.33$), N_{CaO} should be equal to about 8. This value was in accordance with results of previous XRD measurements [12] (cf. Figure 7). However, the present experiment reveals an N_{CaO} number of about 6, the same value as found at the minimal packing density ($y = 0.5$) and just above it ($y = 0.66$). Such as the Ca–O distances do not much vary in this compositional range, this finding must assumed to be correct. Hence, in the glass of 25 mol% CaO the largest possible O_{DB} coordination is not satisfied and some of the O_{DB} atoms remain without a cation neighbour. Obviously, not all O_T atoms can approach the Ca^{2+} cations in such inflexible networks which are dominated by Q^3 groups.

The curves of N_{CaO} and M_{TO} values cross at $y = 0.5$ (cf. Figure 7). Thus, the calcium ultraphosphate glass of $y = 0.5$ is dominantly constituted from CaO_6 and PO_4 polyhedra which are linked by vertices, i.e. the O atoms are positioned on bridging positions, the O_B at P–O–P and the O_T at Ca–O–P bridges. Step by step, if $y = 0.5$ is exceeded, the Ca–O–P bridges are lost. This process is attended by an increase of N_{CaO} and r_{CaO} values (cf. Figure 7). Here N_{CaO} increases though M_{TO}, the number of available terminal oxygen atoms per cation, is diminished. The enhanced flexibility of the network which is formed from a large fraction of Q^2 groups and without any strong topological order required by Ca–O–P bridges enables the increase of N_{CaO}.

The successful combination of neutron diffraction and XRD data to determine Me–O coordination numbers is limited to glasses with a reasonable amount of metal oxide. It would have no meaning to study N_{CaO} values in glasses with less than 25 mol% CaO.

5. Conclusions

The existence of the PO_4 tetrahedra and the formation of definite numbers of links between them are known facts of the structure of phosphate glasses. The results of the diffraction methods here presented and the subsequent discussion, where distances of related crystals and data from MO calculations were included, extends the knowledge on further structural details.

For the first time the splitting of the P–O distance peak into contributions from the bonds of the phosphorus to the terminal (O_T) and the bridging (O_B) oxygen atoms was obtained in ultraphosphate glasses. The varying fractions of these bonds corroborate the depolymerization scheme of the network. The mean P–O bond lengths are almost invariable versus the metal oxide content, while the increase of the $P–O_T$ and $P–O_B$ distances compensates for the growing fraction of the shorter bonds, i.e. those to the O_T atoms. In general, this agrees with the behaviour of bonds in the related crystals and in clusters obtained by ab initio calculations.

From considerations on structural details in the crystals and clusters the following conclusions were drawn: Contrary to a nominal distinction of $P–O_T$ distances in Q^3 and Q^2 groups, any differences of lengths are smeared out under the attack of the modifier cations. The transfer of electron density from the

Q^2 to the Q^3 group reflects the corresponding mechanism. Thus, the improvement of the local charge compensation favours links between pairs of unlike Q^n. Thereby the $P-O_B$ bond in a Q^2 is lengthened while the corresponding bond in the Q^3 is shortened. However, these distances could not be distinguished in the glasses studied.

Of special interest in phosphate glasses is the compositional point where the number of available terminal oxygen atoms per modifier cation is equal to the Me–O coordination number. Definite changes of N_{MeO} values in the vicinity of this point would indicate a stabilization of Me–O–P bridges. With a value N_{CaO} of about 6 obtained at this composition with $n(CaO)/n(P_2O_5) = 0.5$ and just below and above it a stabilization of Ca–O–P bridges by the calcium cations is not confirmed. On the other hand, the zinc atoms change their oxygen coordination number from 6 to 4 according to the decreasing number of available terminal oxygens.

Acknowledgements

The financial support of the Deutsche Forschungsgemeinschaft (grant WA 842/1–2) is gratefully acknowledged.

[1] R. Gresch, W. Müller-Warmuth, and H. Dutz, J. Non-Cryst. Solids **34,** 127 (1979).
[2] R. K. Brow, D. R. Tallant, J. J. Hudgens, S. W. Martin, and A. D. Irwin, J. Non-Cryst. Solids **177,** 221 (1994).
[3] R. K. Brow, J. Non-Cryst. Solids **194,** 267 (1996).
[4] J. R. Van Wazer, in Phosphorus and its Compounds, Vol. **1** (Interscience, New York 1958).
[5] P. Losso, B. Schnabel, C. Jäger, U. Sternberg, D. Stachel, and D. O. Smith, J. Non-Cryst. Solids **143,** 265 (1992).
[6] K. Suzuki and M. Ueno, J. Physique (Paris) **46,** C8-261 (1985).
[7] U. Hoppe, G. Walter, D. Stachel, and A. C. Hannon, Z. Naturforsch. **51a,** 179 (1996).
[8] U. Hoppe, G. Walter, D. Stachel, and A. C. Hannon, Z. Naturforsch. **50a,** 684 (1995).
[9] U. Hoppe, J. Non-Cryst. Solids **195,** 138 (1996).
[10] U. Hoppe, G. Walter, R. Kranold, and D. Stachel, Z. Naturforsch., submitted.
[11] U. Hoppe, G. Walter, and D. Stachel, Silikattechnik **41,** 227 (1990).
[12] U. Hoppe, G. Walter, R. Kranold, D. Stachel, and A. Barz, J. Non-Cryst. Solids **192, 193,** 28 (1995).
[13] U. Hoppe, D. Stachel, and D. Beyer, Physica Scripta T **57,** 122 (1995).
[14] K. Meyer, A. Barz, and D. Stachel, J. Non-Cryst. Solids **191,** 71 (1995).
[15] A. C. Hannon, W. S. Howells, and A. K. Soper, IOP Conf. Series **107,** 193 (1990).
[16] J. Waser and V. Schomaker, Rev. Mod. Phys. **25,** 671 (1953).
[17] A. C. Wright and A. J. Leadbetter, Phys. Chem. Glasses **17,** 122 (1976).
[18] M. Jansen and B. Lüer, Z. Kristallogr. **177,** 149 (1986).
[19] El H. Arbib, B. Elouadi, J. P. Chaminade, and J. Darriet, J. Solid State Chem., at press.
[20] D. Stachel, I. Svoboda, and H. Fuess, Acta Cryst. C **51,** 1049 (1995).
[21] C. Bäz-Dölle, D. Stachel, I. Svoboda, and H. Fuess, Z. Kristallogr. **203,** 282 (1993).
[22] I. Tordjman, M. Bagieu-Beucher, and R. Zilber, Z. Kristallogr. **140,** 145 (1974).
[23] K. R. Albrund, R. Attig, J. Feener, J. P. Jeser, and D. Mootz, Mater. Res. Bull. **9,** 129 (1974).
[24] D. Stachel, H. Paulus, I. Svoboda, and H. Fuess, Z. Kristallogr. **202,** 117 (1992).
[25] M. Schneider, K. H. Jost, and P. Leibnitz, Z. Anorg. Allg. Chem. **527,** 99 (1985).
[26] T. Uchino and Y. Ogata, J. Non-Cryst. Solids **181,** 175 (1995).
[27] V. Gutmann, in The Donor – Acceptor Approach to Molecular Interactions, Plenum Press, New York 1978, pp. 4–16.
[28] T. Uchino, T. Sakka, Y. Ogata, and M. Iwasaki, J. Phys. Chem. **96,** 2455 (1992).
[29] J. A. Duffy, G. D. Chryssikos, and E. I. Kamitsos, Phys. Chem. Glasses **36,** 53 (1995).
[30] C. Jäger, M. Feike, R. Born, and H. W. Spiess, J. Non-Cryst. Solids **180,** 91 (1994); and R. Born, M. Feike, C. Jäger, and H. W. Spiess, Z. Naturforsch. **50a,** 169 (1995).
[31] H. Reiss and D. Stachel, in 4th Internat. Otto Schott Colloquium, Wissenschaftliche Beiträge der Friedrich Schiller Universität Jena, Jena 1990, p. 112.